Acta Scientiarum

http://www.uem.br/acta
ISSN printed: 1806-2563
ISSN on-line: 1807-8664
Doi: 10.4025/actascitechnol.v37i4.27519

Dissipated energy in tapping mode by the atomic force microscope

Gerson Anderson de Carvalho Lopes[1] and Henrique Duarte da Fonseca Filho[2*]

*[1]Centro de Educação, Engenharia e Matemática, Universidade Estadual do Amapá, Macapá, Amapá, Brazil. [2]Laboratório de Ciências dos Materiais, Departamento de Física, Universidade Federal do Amapá, Rodovia Juscelino Kubitschek de Oliveira, Km 2, Macapá, Amapá, Brazil. *Author for correspondence. E-mail: hdf_filho@unifap.br*

ABSTRACT. Dissipated energy measurements between a tip of an AFM and a sample have been used to analyze variations in mechanical and tribological properties of materials, using tapping mode AFM to generate topography and phase contrast images. Furthermore it's possible to perform indentations in the material with this operation mode and to create micro-controlled defects, in diameter and depth, to growing of quantum dots in semiconductor materials. In this paper, we discuss the fundamentals of this technique.

Keywords: phase contrast, plastic deformations, tip, nanoscale.

Energia dissipada em modo tapping pelo microscópio de força atômica

RESUMO. As medições da energia dissipada entre a ponta de um AFM e a superfície de uma amostra foram usadas para analisar as variações nas propriedades mecânicas e tribológicas dos materiais, utilizando o modo de tapping do AFM para obter imagens de topografia e de contraste de fase. Além disso, foi possível realizar indentações no material através desse modo de operação e criar defeitos micro controlados, em diâmetro e profundidade, para o crescimento de pontos quânticos em materiais semicondutores. Neste artigo, discutimos os fundamentos dessa técnica.

Palavras-chave: contraste de fase, deformações plásticas, ponta, nanoescala.

Introduction

Atomic Force Microscope (AFM) has been used as a powerful tool for the study of surface properties at the nanoscale (HYON et al., 2000; DU et al., 2001). Besides, AFM nanolithography has proven to be a unique tool for material structuring and patterning with nanometer precision. AFM arose in 1986 for use as a microscope to directly image the surface morphology with atomic and molecular resolution (BINNIG et al., 1986). The morphological image of a surface is obtained by recording and regulating the forces felt by a probe as it scans the surface. AFM can be used to study both insulating and conducting materials, and can be operated in liquid, air or vacuum. This equipment consists of a probe in form of a little stem or rod, called cantilever, which has a tip with nanometrical dimensions, mounted at its extremity, and moves along the sample surface, 'feeling' the tip-sample interaction force intensity.

As the probe scans the sample surface, the intensity of the interaction varies, and the cantilever then undergoes deflections, which are perceived through the variation in the reflection angle of a laser beam falling over the upper surface of the rod, coming from a photodiode, and is detected by a photo detector.

The AFM captures the deflection information of the cantilever and transmits it, through an electronic module, to the computer, which transforms the values of deflection into a range of pixels, constructing in this way a z (x, y) matrix, where z is the altitude of the sample at the point given by coordinates x and y.

The deflection signal is also relayed from the electronic module to the microscope headstock, by a PID system control, which nanometrically adjusts the tip-sample distance for the interaction force to remain constant.

The objective of this review is to present the new developments in applications of nanolithography using an AFM and the consequences of dissipated energy in tapping mode. It is useful to provide a short introduction to the concept of the AFM and some characteristics of the instruments used. Quantitative and qualitative determination about nanoindentations and dissipated energy using this technique are presented.

Mode of operation of the AFM

The AFM can operate basically in three different modes, namely, contact, non-contact, and intermittent contact (tapping), the latter also called

amplitude modulation mode. The primary difference between these three modes of operation refers to what region of the regime of forces the tip-sample interaction is happening at the time of scanning.

Figure 1 shows the variation in the intensity of the interaction force between two isolated atoms according to separation distance, following the Lennard-Jones (LJ) model, which is expressed by Equation 1 (NUSSENZVEIG, 2002).

$$F_{LJ} = -24\varepsilon\left[2\left(\frac{\sigma^{12}}{z^{13}}\right) - \left(\frac{\sigma^{6}}{z^{7}}\right)\right] \quad (1)$$

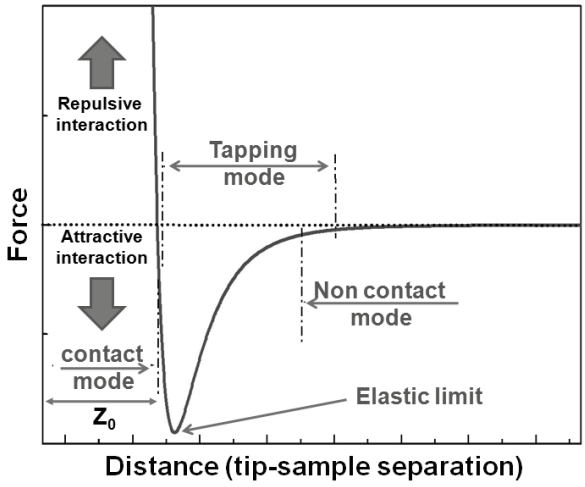

Figure 1. Model for the tip-sample interaction, z_0 is the equilibrium distance.

In Equation 1, z is the separation distance between two single atoms, σ and ε are, respectively, the average radius and a constant, which depends on the properties of each atom.

If the tip is far from the sample, the forces that prevail between it and the sample are mostly Van der Waals forces, which are essentially attractive (non-contact mode), but if the tip is touching the sample during the scanning (contact mode), the predominant forces are repulsive (BUTT et al., 2005). This phenomenon is due to the Pauli exclusion principle, due to the superposition of atomic orbital of atoms in the very end of the tip with the ones of the surface.

The third operation mode, emphasized herein, is called tapping, because the tip is placed in oscillation with an equilibrium separation (distance between the sample and the base of the cantilever) smaller than the amplitude, so that the tip reaches the surface once every cycle at one end of the oscillation (BABCOCK; PRATER, 2010).

This mode was introduced to the AFM technique to minimize deformations of the tip and the sample and also to increase the spatial resolution of the images (ANCZYKOWSKI et al., 1999), and has become popular among researchers mainly due to its ability to perform images of surfaces with low stiffness, since lateral forces that may cause damages to the sample are diminished in comparison with contact mode (GARCÍA et al., 1998; HÖLSCHER; SCHWARZ, 2007).

Several dynamic models for the cantilever operating in tapping mode consider it as a non-linear driven harmonic oscillator with damping (TAMAYO; GARCÍA, 1996), whose motion is governed by the following Equation 2:

$$m\frac{d^2z}{dt^2} = -kz - \frac{m\omega_0}{Q}\frac{dz}{dt} + F_0\cos(\omega t) + F(z, z_c) \quad (2)$$

In the Equation above, k, ω, ω_0, $m$and$Q$are the elastic constant of the cantilever, the oscillation frequency of the driver, the resonant frequency, the mass and quality factor of the cantilever, respectively. The above Equation is derived from Newton's second law, with the term proportional to the velocity corresponding to viscous damping of the environment in which cantilever is immersed (which may be air or a liquid), and the term proportional to the deflection is the restoring force. The sinusoidal term represents the excitation signal applied to the cantilever by the electronic module and the last term on the right side represents the interaction between the tip and the surface.

The tip-surface interaction term is written in two different ways considering the instants at which cantilever is touching the surface and those ones where the two materials are apart. When the probe is far from the sample, the interaction force is modeled by the van der Waals interactions between a sphere and a flat surface (Equation 3).

$$F(z, z_c) = -\frac{AR}{6(z_c + z)^2} \quad z_c + z \leq a_0 \quad (3)$$

For the region at which the tip touches the sample, the interaction is modeled by the indentation force derived from Hertz model – Equation 4 – (ISRAELACHVILLI, 2011).

$$F(z, z_c) = -\frac{A}{6a_0} + \frac{4E\sqrt{R}}{3-3\nu^2}(a_0 - z - z_c)^{3/2} \quad + \leq_0 \quad (4)$$

Then, the working principle of AFM nanolithography is based on the interaction between the probe and substrate. The nanoindentation process is performed with the use of a program supported by the microscope software that precisely

controls the movement of the microscope tip. At pre-defined points, computer orders probe to stop for few seconds and raise its oscillation amplitude, so that the stem have sufficient energy to break the edges of the sample lattice, and thus a defect is created on the surface.

After this, the cantilever continues to scan until reaching another point set by the software to perform a new nanoindentation. Thus, it is constructed a pattern of defects on the surface of the semiconductor material, as shown in Figure 2, wherein nanoindentations were carried out with different amplitude values. The experiment conducted by Fonseca Filho et al. (2007) found a direct relationship between the vibration amplitude and the depth of deformation.

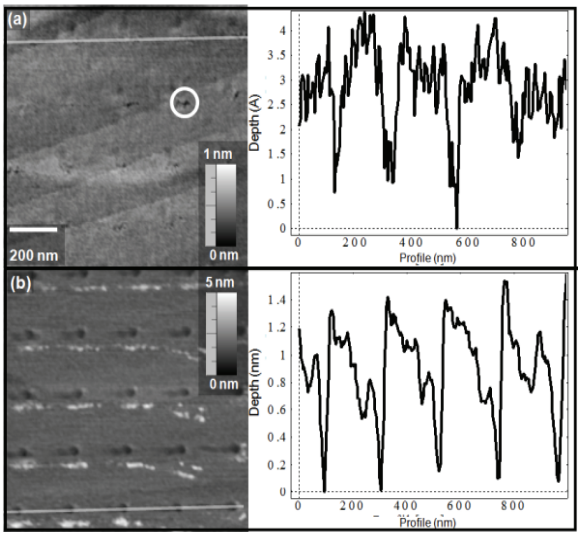

Figure 2. AFM images created with values of vibration amplitude of (a) 7.5 volts and (b) 15 volts and the respective profiles of the indicated lines. In (a) created defects are irregular as highlighted by the white circle, for example, unlike (b) (FONSECA FILHO et al., 2007).

Therefore, the deformations induced in the material are no longer purely elastic, but also plastic. Thus, the last term of Equation 1 must be modified for the case where the tip indents the surface plastically.

Contact mechanics

Theories on contact mechanics have been applied with success to the study of elastic properties of the samples studied with AFM, though, studies hold only to momentary deformations introduced by the tip in the scanning process, without mentioning the plastic deformations caused by nanoindentations with tapping mode.

These theories intend to explain how the contact area and deformation vary with the applied pressure on the bodies. Some of the most used models are discussed below, including: Hertz model, DMT and JKR (JOHNSON, 1985).

Hertz model:

It is the simplest and most used in the works dealing with mechanical deformations. This model considers the contact between two homogeneous and isotropic spheres, neglecting the van der Waals interactions and friction forces between the surfaces. Often one makes one of the spheres to have an infinite radius of curvature, so that the contact is that of a sphere and a flat surface.

According to Equation 5, the contact radius a and the deformation δ are given in function of the applied force F by:

$$a = \left(\frac{RF}{E_{tot}}\right)^{\frac{1}{3}} \quad \delta = \left(\frac{F^2}{RE_{tot}^2}\right)^{\frac{1}{3}} \tag{5}$$

where:
R is the radius of the sphere and is the reduced Young modulus equal, according to Equation 6:

$$\frac{1}{E_{tot}} = \frac{3}{4}\left(\frac{1-\nu_a^2}{E_a} + \frac{1-\nu_e^2}{E_e}\right) \tag{6}$$

where:
ν_a, ν_e, E_a, E_e are the Poisson coefficients and the Young modulus for the sample and the sphere, respectively (TIMOSHENKO; GOODIER, 1951).

DMT model:

Differently from the Hertz model, this theory considers also the intermolecular interactions between the sphere and the plane. The contact radius and deformation are, in this way, given by Equations 7 and 8:

$$a = \left(\frac{R(F+2\pi RW)}{E_{tot}}\right)^{\frac{1}{3}} \tag{7}$$

$$\delta = \left(\frac{(F+2\pi RW)^2}{RE_{tot}^2}\right)^{\frac{1}{3}} \tag{8}$$

where:
W is the adhesion work per unit area.

JKR model:

The difference of this model is the inclusion of the adhesion contribution to the tip-sample interaction. Thus the contact radius and deformation become (Equation 9):

$$a = \left(\frac{R\left(F + 3\pi RW + \sqrt{6\pi RWF + (3\pi RW)^2}\right)}{E_{tot}} \right)^{\frac{1}{3}} \delta = \frac{2}{3}\sqrt{\frac{6\pi Wa}{E_{tot}}} \quad (9)$$

Plastic deformation

Some studies of plastic deformations have recently emerged, including some dealing with nanoindentations in semiconductor materials, more specifically, InP (HUANG et al., 2013). It is shown, through the analysis of force-distance curves, that InP deformation occurs in a discontinuous manner, with a phenomenon known as pop-in in the regions where there is disruption of the crystal planes in the material.

This process of deformation differs from that of amorphous materials, like polymer films, where there is also a change in the slope of force-distance curves at the moment of the beginning of plastic deformations, but this variation occurs continuously.

Cappella et al. (2005) elaborated a model of deformation that considers a polymer film as a bi-layer composed of two materials with different elasticity modulus, so that, when hitting the harder material, deformation occurs differently, reproducing the variation in slope observed in the curve shown before.

For a crystalline material, it is considered several stages, corresponding to the regions between the pop-ins, each one described by a curve similar to that of a polymer bi-layer, but separated by the discontinuities of pop-ins.

Thus, plastic deformation is modeled separated for each crystalline plane. Calculating the work performed, through the integration over a cycle of the product of the force exerted on the material and the deformation, there is an estimation of the dissipated energy in the process of nanoindentation.

Dissipated energy

To obtain an experimental value of dissipated energy during the nanoindentation process, in order to compare it to the theoretical model, one can proceed in two different manners: force-distance curves or phase contrast images.

The analysis of force-distance curves, such as in figure 3, can provide an estimation of the energy spent in the nanoindentation, calculating the area between the approaching and retracting curves (A1), known as hysteresis loop, which is characteristic of non-conservative processes. The area below the retracting curve represents the amount of energy provided by the cantilever to the sample that was recovered when undoing the perforation movement in the surface.

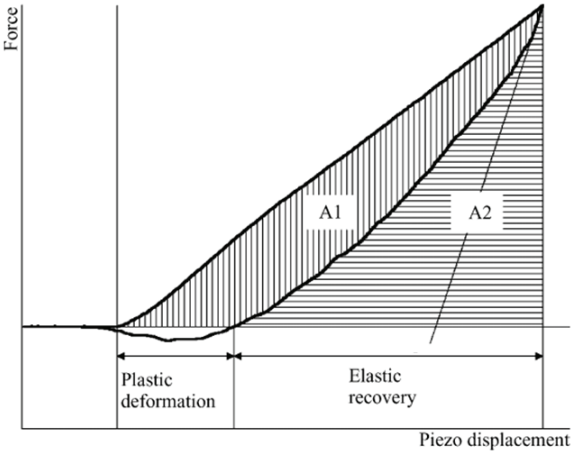

Figure 3. Force applied by the cantilever on the sample, highlighting the way to estimate dissipated energy in the indentation calculating the area between both curves (BUTT et al., 2005).

However, these curves are provided by a nanoindentator, and not by an AFM operating in tapping mode. There is another way to estimate the energy loss using AFM, which uses the phase contrast images.

Phase contrast or phase shift is the denomination for the difference between the phase angle of the excitation signal and the phase angle of the cantilever response (ANCZYKOWSKI et al., 1999). Some studies have shown that phase contrast images are related to the energy dissipation in the process of imaging the surface, once which has already be shown that inelastic interactions are responsible for the appearance of phase shift (TAMAYO; GARCÍA, 1998). The dependence of the variation in the phase angle with the energy dissipated can be calculated by a simple model (CLEVELAND et al., 1998; ANCZYKOWSKI et al., 1999).

To construct this model, it is considered that, in the steady state, the motion of the cantilever is approximately sinusoidal. The movement of the driver is governed by the Equation 10:

$$z_d(t) = A_d \cos(\omega t) \quad (10)$$

While the motion of the end of cantilever is governed by the Equation 11:

$$z(t) = A \cos(\omega t + \varphi) \quad (11)$$

where:
in this Equation, φ is the phase difference between the driver and the stem response.

In steady state, the energy, and consequently, the power provided to the cantilever equals the loss due to damping and the dissipation by the sample (Equation 12).

$$\overline{P_I} = \overline{P_A} + \overline{P_D} \quad (12)$$

The average power transmitted by the external force is the integral, among a cycle, of the product of this force by the velocity of the driver, distributed over the period (Equations 13 and 15).

$$\overline{P_I} = \frac{1}{T}\int_t^{t+T} F\dot{z_d} = \quad (13)$$

$$\frac{\omega}{2\pi}\int_t^{t+\frac{2\pi}{\omega}} k[z(t) - z_d(t)]\dot{z_d}(t) = \quad (14)$$

$$\frac{1}{2}kA_dA\omega\sin\varphi \quad (15)$$

The viscous damping of environment is well modeled by a force proportional to velocity. Similarly, it can be calculated the average power dissipated over a cycle (Equation 16).

$$\overline{P_A} = \frac{1}{T}\int_t^{t+T} F\dot{z_d} = \frac{\omega}{2\pi}\int_t^{t+\frac{2\pi}{\omega}} -b\dot{z}\dot{z_d} = \frac{1}{2}bA^2\omega^2 \quad (16)$$

Solving for the power dissipated in the tip-sample interaction, and considering that $b = k/Q\omega_0$, Q is the quality factor of cantilever, we have (Equation 17 and 18):

$$\overline{P_D} = \overline{P_I} - \overline{P_A} = \quad (17)$$

$$\frac{1}{2}\frac{kA^2\omega}{Q}\left[\frac{QA_d\sin\varphi}{A} - \frac{\omega}{\omega_0}\right] \quad (18)$$

Therefore, it turns out that the sine of the phase difference between the oscillator and the cantilever response is directly proportional to the energy loss per cycle in tip-sample interaction.

Commonly, the frequency ω is chosen to be ω_0 and, in this case, some simplifications can be done, because we can define $A_0 = QA_d$, then we have Equation 19:

$$\overline{P_D} = \frac{1}{2}\frac{kA^2\omega_0}{Q}\left[\left(\frac{A_0}{A}\right)\sin\varphi - 1\right] \quad (19)$$

If there is no energy loss, amplitude and phase are not independent (Equation 20):

$$\varphi = \sin^{-1}\left(\frac{A}{A_0}\right) \quad (20)$$

However, these energy dissipations occur at the time of imaging, and are not the energies spent to create a defect on the surface.

Thus, phase contrast images can be interpreted as dissipation maps during the scanning. This prediction, done firstly by Cleveland et al (1998), was confirmed by Tamayo et al (1998) when performing phase contrast images on samples with heterogeneous surfaces, consisting of some spots of purple membrane (PM) deposited over highly oriented pyrolytic graphite (HOPG) substrate (Figure 4).

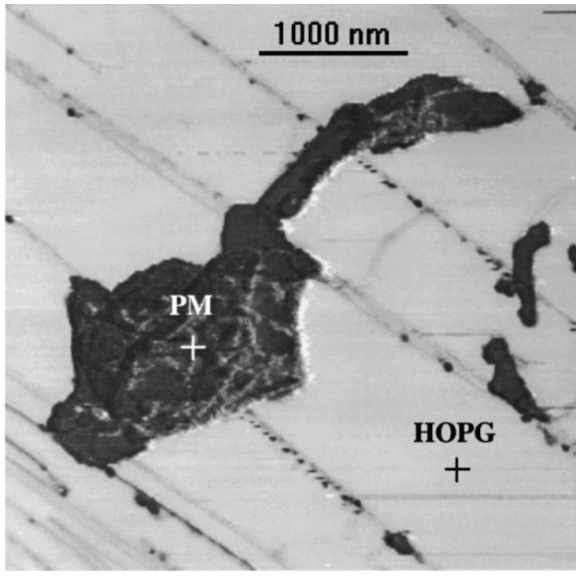

Figure 4. Phase-contrast image of a purple membrane on graphite. The phase shift is 10.5±0.5° higher on graphite than on the membrane. This shift is independent of the number of membranes piled up. The thickness of a single membrane is about 5 nm. A_0 = 43 nm, A_t = 34 nm, k = 45 N m^{-1}, f = f_0 = 356 KHz, and Q = 270. The crosses mark the sites where the force curves were measured (TAMAYO and GARCÍA, 1998).

These authors did some measurements of energy dissipated on the sample through the force-distance curves (Figure 5), obtained by approaching and retracting the cantilever over the surface at the points marked with the crosses in the previous figure. The feedback mechanism is turned out, and the deflection of cantilever is measured in approximation and retracting the surface with 40 Hz. Then, the force is obtained by multiplying the deflection by the elastic constant of the cantilever (Figure 5). It is assumed that the force curve does not depend on the load-unload frequency.

The results show that elastic deformations prevail in the region of repulsive forces, once that approximation and retracting curves superpose. One can also verify that the energy loss is dominated by the action of adhesion and capillarity forces, because the larger area between both curves is in the attractive region.

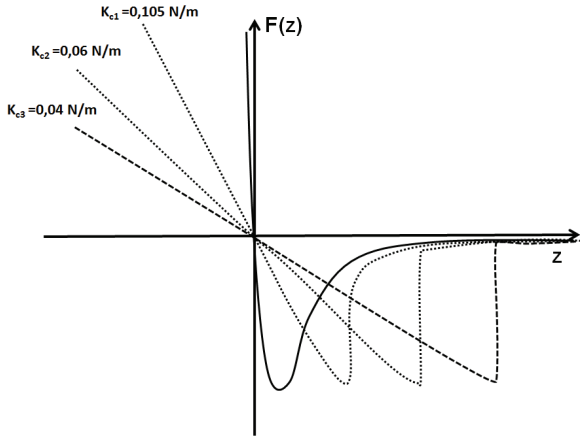

Figure 5. Force-displacement curves (broken lines) obtained with three cantilevers of different elastic constants Kc >> Ks. The continuous line is the tip-sample interaction, modeled with a Lennard-Jones interaction with A = 10^{-77} Jm^6 and B = 10^{-134} Jm^{12} (CAPELLA; DIETLER, 1999).

It can be inferred data about deformation using phase contrast images, since phase contrast arises due to changes in the elastic properties of the sample at every point on the surface (BUTT et al., 2005). Plastically deformed samples present variations in Young modulus at the region of deformation, which are captured at the moment of obtaining phase contrast images. This occurs because the plastically modified part of the sample leads the cantilever to vibrate in a different way when the probe touches the surface, once this region is usually more rigid than the rest of the material (TAMAYO; GARCÍA, 1997).

Conclusion

This research presented how the AFM tapping mode can be used to perform indentations on the surface of samples, being important to determine the mechanism of the energy loss during the generation of the defects, once it determines the dimensions, diameter and depth of the defects, which are, in turn, crucial for the growth of quantum dots over the defects.

The study of energy dissipations is important even in the case of plastic deformations occurring during the scanning of the sample. It was demonstrated the important role played by tapping mode in the study of energy dissipations for materials, science and applications.

References

ANCZYKOWSKI, B.; GOTSMANN, B.; FUCHS, H.; CLEVELAND, J. P.; ELINGS, V. B. How to measure energy dissipation in dynamic mode atomic force microscopy. **Applied Surface Science**, v. 140, n. 3-4, p. 376-382, 1999.

BABCOCK, K. L.; PRATER, C. B. **Phase imaging**: beyond topography. Santa Barbara: Digital Instruments, 2010.

BINNIG, G.; QUATE, C. F.; GERBER, C. Atomic force microscope. **Physics Review Letters**, v. 56, n. 9, p. 930-933, 1986.

BUTT, H.-J.; CAPPELLA, B.; KAPPL, M. Force measurements with the atomic force microscope: Technique, interpretation and applications. **Surface Science Reports**, v. 59, n. 1-6, p. 1-152, 2005.

CAPELLA, B.; DIETLER, G. Force-distance curves by atomic force microscopy. **Surface Science Reports**, v. 34, n. 1-3, p. 1-104, 1999.

CAPPELLA, B.; KALIAPPAN, S. K.; STURM, H. Using AFM force-distance curves to study the glass-to-rubber transitions of amorphous polymers and their elastic-plastic properties as a function of temperature. **Macromolecules**, v. 38, n. 5, p. 1874-1881, 2005.

CLEVELAND, J. P.; ANCZYKOWSKI, B.; SCHMID, A. E.; ELINGS, V. B. Energy dissipation in tapping-mode atomic force microscopy. **Applied Physics Letters**, v. 72, n. 20, p. 2613-2615, 1998.

DU, B.; VANLANDINGHAM, M. R.; ZHANG, Q.; HE, T. Direct measurement of plowing friction and wear of a polymer thin film using the atomic force microscope. **Journal of Materials Research**, v. 5, n. 16, p. 1487-1492, 2001.

FONSECA FILHO, H. D.; PRIOLI, R.; PAMPLONA, M.; LOPES, A. S.; SOUZA, P. L.; PONCE, F. Growth of InAs nanostructures on InP using atomic-force nanolithography. **Applied Physics A**, v. 89, n. 4, p. 945-949, 2007.

GARCÍA, R.; TAMAYO, J.; CALLEJA, M.; GARCÍA, F. Phase contrast in tapping-mode atomic force microscopy. **Applied Physics A.**, v. 66, n. 6, p. 309-312, 1998.

HÖLSCHER, H.; SCHWARZ, U. D. Theory of amplitude modulation atomic force microscopy with and without Q-control. **International Journal of Non-linear mechanics**, v. 42, n. 4, p. 608-625, 2007.

HUANG, J. Y.; PONCE, F. A.; CALDAS, P. G.; PRIOLI, R.; ALMEIDA, C. M. The effect of nanoscratching direction on the plastic deformation and surface morphology of InP crystals. **Journal of Applied Physics**, v. 114, n. 20, p. 203-503, 2013.

HYON, C. K.; CHOI, S. C.; SONG, S. H.; HWANG, S. W.; SON, M. H.; AHN, D.; PARK, Y. J.; KIM, E. K. Application of atomic-force-microscope direct patterning to selective positioning of InAs quantum dots on GaAs. **Applied Physics Letters**, v. 16, n. 77, p. 2607-2609, 2000.

ISRAELACHVILLI, J. **Intermolecular and surface forces**. 3rd. ed. Londres: Academic Press, 2011.

JOHNSON, K. L. **Contact mechanics**. Londres: Cambrige University Press, 1985.

NUSSENZVEIG, H. M. **Curso de física básica** - mecânica. 4. ed. São Paulo: Edgard Blücher, 2002.

TAMAYO, J.; GARCÍA, R. Deformation, contact time, and phase contrast in tapping mode scanning force

microscopy. **Langmuir**, v. 12, n. 18 p. 4430-4435, 1996.

TAMAYO, J.; GARCÍA, R. Effects of elastic and inelastic interactions on phase contrast images in tapping-mode scanning force microscopy. **Applied Physics Letters**, v. 71, n. 16, p. 2394-2396, 1997.

TAMAYO, J.; GARCÍA, R. Relationship between phase shift and energy dissipation in tapping-mode scanning force microscopy. **Applied Physics Letters**, v. 73, n. 20, p. 2926-2928, 1998.

TIMOSHENKO, S.; GOODIER, J. N. **Theory of elasticity**. New York: McGraw-Hill Book Company, 1951.

Received on April 24, 2015.
Accepted on September 1, 2015.